Received: 19 June 2018 | Revised: 6 August 2018 | Accepted: 10 September 2018

DOI: 10.1002/bio.3558

RESEARCH ARTICLE

WILEY LUMINESCENCE
The Journal of Biological and Chemical Luminescence

Application of modified mesoporous boehmite (γ-AlOOH) with green synthesis carbon quantum dots for a fabrication biosensor to determine trace amounts of doxorubicin

Behzad Rezaei | Zahra Hassani | Marzieh Shahshahanipour | Ali A. Ensafi | G. Mohammadnezhad

Department of Chemistry, Isfahan University of Technology, Isfahan, Iran

Correspondence
Behzad Rezaei, Department of Chemistry, Isfahan University of Technology, Isfahan, 83111, Iran.
Email: rezaei@cc.iut.ac.ir

Funding information
Isfahan University of Technology (IUT) Research Council, Center of Excellence in Sensor and Green Chemistry

Abstract

An important form of carbon nanoparticles that are used for a wide range of applications, are carbon dots (CDs). In this study, a very easy, in expensive and green process was described for the preparation of CDs by using hydrothermal treatment of Tragacanth Gum (TG). A rapid assay for the determination of trace amounts of an anticancer medication doxorubicin (DOX) was developed, based on the quenching of the CDs derived from their aggregation. Electrostatic interaction between CDs and DOX could lead to fluorescence quenching. The optimized biosensor showed a detection range from 1 to 400 ng mL^{-1} and a limit of detection of 0.4 ng mL^{-1}. In the following, the synthesized CDs modified the Boehmite (Boh) mesoporous surface based on hydrogen bonding. The Boh has been used as supports and ideal hosts in this method, in which the particle size distribution of CDs in the pores of Boh is limited and they have controlled pore sizes. Accordingly, the surface-to-volume ratio and the presence of high-volume pores increased the longevity and sustainability of CDs; also prevented the aggregation of the CDs and improved their photo stability. The advantages of Boh are large pore volume, high surface area, and narrow size distribution. Variable factors influencing optical sensor response in DOX measurement were evaluated and optimized. In optimal conditions, the linear range was calculated from 1 to 500 ngmL^{-1} and the detection limit was 0.2 ng mL^{-1}. The sensors were used for measuring DOX in human blood plasma.

KEYWORDS

Boehmite, doxorubicin, green synthesized carbon dots, nano sensor

1 | INTRODUCTION

The carbon dots (CDs) are a recent shape of carbon nano compounds that were discovered fortuitously in the filtration of a single-walled carbon nanotube.[1] Since the CDs are non-toxic, have good biocompatibility, excellent water solubility, high stability, small size (< 10 nm) and inexpensive features, they are attractive, especially for in vivo and in vitro bio analytical diagnostics, photo catalysis, in medicine, as sensors and drug delivery.[2,3] The variation in fluorescence is observed dependent on the exaltation wavelength.[3] The CDs were synthesized by various methods such as laser ablation,[4] chemical oxidation[5] and hydrothermal method.[6] The one-step hydrothermal method due to the simplicity and low cost of the method has attracted the attention of researchers in recent years.[7] The CDs were

synthesized from a low cost, available green plant by the hydrothermal method. The mentioned plant was Tragacanth Gum (TG).

The plant TG mostly grows in mountainous areas of Iran and Turkey. Owing to its biological properties, it has been used for bio-medical applications. In this work, for the first time, TG is used as a carbon source for the preparation of CDs. TG is usually classified with a 'soluble' part: tragacanthin and an 'insoluble' part: bassorin. During acid hydrolysis, TG usually generates sugars of D-galacturonic acid, D-galactose, L-fucose (6-deoxy-L-galactose), D-xylose, L-arabinose and L-rhamnose.[8] TG is utilized as the main substitute in many applications and the gum has been used a lot of times as an additive, thickener, emulsifier and hanging agent in pharmaceutical, diet and beautifying artifacts, in addition to other practical uses based on its great viscosity at insignificant concentrations.[9]

First, hydrolysis and decomposition of carbohydrates are accomplished, resulting in water loss and carbohydrate production. During the polymerization and condensation of these products, The condensation of these polymer compounds leads to the formation of aromatic clusters. Finally, nuclear explosions occurs, and eventually, the CDs are synthesized.[6]

Doxorubicin (DOX) is an essential component of the anthracylinic group and it is an important drug for treatment of cancers such as breast carcinoma, thyroid carcinoma, bronchogenic carcinoma, aggressive lymphoma, gastric carcinoma and others.[10] Irreversible cardiotoxicity, myelosuppression, marrow suppression and hypoalbuminemia were observed in patients with the use of high doses of DOX. Therefore, detection of trace amounts of DOX is of special importance for hospitals and laboratories.[11]

For the earlier mentioned reasons, precision, rapid and accurate determination of DOX in plasma specimens has warranted much care. Different techniques have been used for the determination of DOX, these include counting high performance liquid chromatography,[12] spectrophotometric,[13] voltammetric,[14] UV absorption,[15] electrochemical sensors[16] and so on. However, the fluorescence assays due to the high sensitivity, fast response, low cost and good reproducibility are good techniques for the determination of DOX.[17]

The aluminum oxyhydroxide, AlO(OH), is well known as Boehmite (Boh), which is a crucial precursor for alumina. The Boh is an important porous material, the pore properties of Boh are important for many industrial applications, such as catalysis application. The CDs doped with Boh have the potential to exhibit novel properties compared with undoped bare Boh. Nano Boh with higher surface zones and large hole volumes (802 m^2 g^{-1}, 2.35 cm^3 g^{-1}, respectively) are purposed as ideal hosts for nanoparticles such as CDs. The CDs are loaded in the pores of Boh with a thin dimension distribution. Therefore, it is found that photoluminescence (PL) of CDs increased after being encapsulated by Boh.[18]

In this study, novel biosensors for DOX detection were expanded based on mechanisms of inner filter effect (IFE) and aggregation. The fluorescence quenching of CDs and CDs/Boh by the addition of DOX were justified based on aggregation and the IFE mechanism, respectively. The IFE is a decline in the fluorescence radiation when the emission and/or absorption spectra of the fluorophore is absorbed by spaces present in the solution.[19] IFEs are defined as apparent decreases in radiation quantum yield and/or alteration of band shapes due to re-absorption of the fluorescence emission, or by absorption of the event radiation by another species than the fluorophore.[20]

Derjaguin–Landau–Verwey–Overbeek (DLVO) theory has been described as the aggregation of aqueous dispersions and the force between charged surfaces. It combines the Van der Waals interactions and the electrostatic repulsion interaction forces dominant over the particles with opposite surface charges in the systems.[21]

Herein, two novel biosensors were successfully used for the determination of trace amounts of DOX. A green, low cost and facile synthesis of CDs, as fluorescent probes were applied by hydrothermal treatment of TG. The advantages of these sensors are that they are affordable and environmentally friendly, have high sensitivity and selectivity with fast responses for the determination of DOX.

2 | EXPERIMENTAL

2.1 | Reagents and chemicals

The TG was obtained from the native grocery shop, after washing with water and drying at room temperature, was powdered and used for the experiments. All chemicals with the maximum grade were obtained from commercial companies (Sigma Aldrich, St Louis, MO, USA and Merck, Darmstadt, Germany). DOX was acquired from Amin Company (Isfahan, Iran). The 0.010 mol L^{-1}universal buffer solution, counting boric acid, citric acid, and phosphoric acid and 0.2 mol L^{-1} sodium hydroxide were prepared. For the synthesis of nano Boh aluminum 2-propoxide, 2-propanol and 2-methoxyethanol were used.[18] (4,5-Dimethylthiazol-2-yl)-2,5-diphenyltetrazolium bromide (MTT) was utilized for the study of biocompatibility of the CDs. The serum tasters were organized from the health care department of the Isfahan University of Technology.

2.2 | Apparatus

A Jasco V-570UV/Vis/NIR spectrophotometer (Tokyo, Japan) was used to record the UV-vis absorbance spectra. Fluorescence emission was measured on a Jasco FP-750 spectrofluorimeter (Tokyo, Japan). Transmission electron microscopy (TEM) images were recorded with a Philips CM30 300 kV (Eindhoven, The Netherlands), X-ray diffraction (XRD) data were collected by a Philips XL-30 ESEM and a dynamic light scattering (DLS) device (Malvern ZEN3600 model, Malvern, UK) was used for the determination of size, distribution and zeta potential. Fourier transform infrared (FT-IR) spectroscopy was measured on a JASCO/680-plusspectrophotometer (Tokyo, Japan). For energy dispersive X-ray (EDX) analyses a Seron AIS 2300 (Uiwang, Korea) was employed. Raman spectroscopy was recorded on a P50C0R20 (Taksan, Kayseri, Turkey). The solution pH was adjusted using a Metrohm pH meter (model 827) with a glass electrode (Corning, NY, USA).

2.3 | Synthesis of CDs and Boh

For the preparation of the CDs, 0.50 g Tragacanth powder was mixed in 40 mL water and solution were severely stirred at laboratory temperature. The mixture was transferred in to a 100 mL autoclave

and placed in a furnace at 180°C for 12 h. Then, the autoclave was cooled to laboratory temperature, the bulky and agglomerated particles separated by centrifuging at 10000 rpm for 20 min, the produced CDs were kept in a dark and cold place until use. Scheme 1 displays the different steps required for the preparation of the CDs. Nano Boh was prepared by the hydrolysis of aluminum 2-propoxide or aluminum 2-methoxyethoxide as the single non-expensive molecular precursors, hydrolysis occurred with the addition of a small amount of an aqueous solution of acetic acid. Then the mixture was refluxed for about 24 h. To remove the surplus quantities of acetic acid and liberated alcohol, the samples were dried under a medium vacuum (70°C) for 3 h.[18]

2.4 | Synthesis of CDs/Boh

The CDs/Boh was synthesized by the reported method in the literature.[22] At room temperature, 4% mass ratio of CDs and Boh were prepared.

The reaction mixture was stirred constantly in the air at laboratory temperature for 8 h. The obtained white material was centrifuged for 15 min (10 000 rpm min^{-1}). The resulting, white material (CDs/Boh) was dried at room temperature.

2.5 | Fluorescent assays

For the determination of DOX, 120 μg mL^{-1} CDs (40 μL of 6.2 mg mL^{-1}) and various concentrations of DOX were added to a universal buffer (pH 5). To measure the fluorescence spectra the solutions were poured into a 1.0 cm quartz cell. For this purpose, the excitation wavelength was set at 400 nm and the responses were recorded in the range of 400 to 700 nm. The slits were set at 10.0 nm. The fluorescence intensities for CDs and CDs/Boh, F_0 (in the absence of DOX) and F (in the presence of DOX) were collected at 489 and 483 nm, respectively, with different concentrations of DOX. For determination of DOX based on CDs/Boh, 120 μg mL^{-1} CDs was replaced by 100 ng mL^{-1} of CDs/Boh.

2.6 | Sample preparation

The serum samples were filtered using a syringe filter (0.45 μm) and were diluted several times with deionized water. The standard addition method was applied for the measurement of DOX. Altered concentrations of DOX were spiked into the serum testers. Then, the 300 μL spiked sample was added to 40 μL CDs. Finally, it was diluted to 2000 μL with universal buffer (pH 5). Next, the fluorescence intensity was collected at 400–700 nm. For CDs/Boh of the sensor, 300 μL spiked sample was added to 200 μL of 1 μg mL^{-1} of CDs/Boh solution instead of CDs and the procedure was repeated as earlier.

2.7 | Quantum yield measurements

Comparing the fluorescent intensity of the synthesized CDs to that of Rhodamine B in ethanol (Φ = 0.31), identifies the quantum yield of CDs.[23] The integrated fluorescent intensity of CDs solutions and Rhodamine B in water were compared based on Equation 1. Both CDs sample and standard solution were excited at 480 nm.

The quantum yield was obtained using Equation 1.

$$Q_x = Q_{st} I_x / I_{st} A_x / A_{st} \eta^2{}_x / \eta^2{}_{st} \quad (1)$$

In Equation I the 'x' and 'st' subscripts denote the sample and standard, respectively, Φ represents the quantum yield, while, A and I are the absorbances and the integrated fluorescence intensities, η represents the refractive index of the water (solvent).

3 | RESULTS AND DISCUSSION

3.1 | CDs and CDs/Boh characterization

3.1.1 | UV

The UV-vis absorption of synthesized CDs, CDs/Boh and TG is shown in Figure 1(a). As can be seen, CDs and CDs/Boh solutions show strong and broad UV-vis absorption peaks at 291 and 350 nm, respectively. CDs/Boh has a higher absorption intensity than bare CDs, which corroborates the n–p transition of the carbonyl. Whereas TG shows a weak peak. The fluorescence spectra of CDs and CDs/Boh at diverse excitation wavelengths were recorded from 260 to 420 nm and are presented in Figure 1(b,c), respectively. In accordance with the characteristics of all known CDs, emission wavelength is dependent on the excitation wavelength. Since there are numerous functional groups and a wide distribution of size, there are different defects (different emission traps) on the outward CDs leading to the creation of different PL properties.[24,25] The emission intensity of CDs/Boh were increased at a different wavelength. Increasing the emission of CDs/Boh is due to the interaction of the AlOOH with oxygen-containing clusters, which results in the change of CDs energy traps.[26]

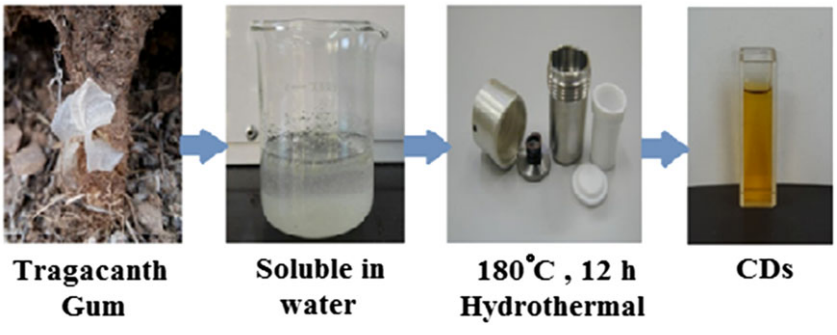

SCHEME 1 Steps of formation of CDs by hydrothermal treatment of Tragacanth Gum

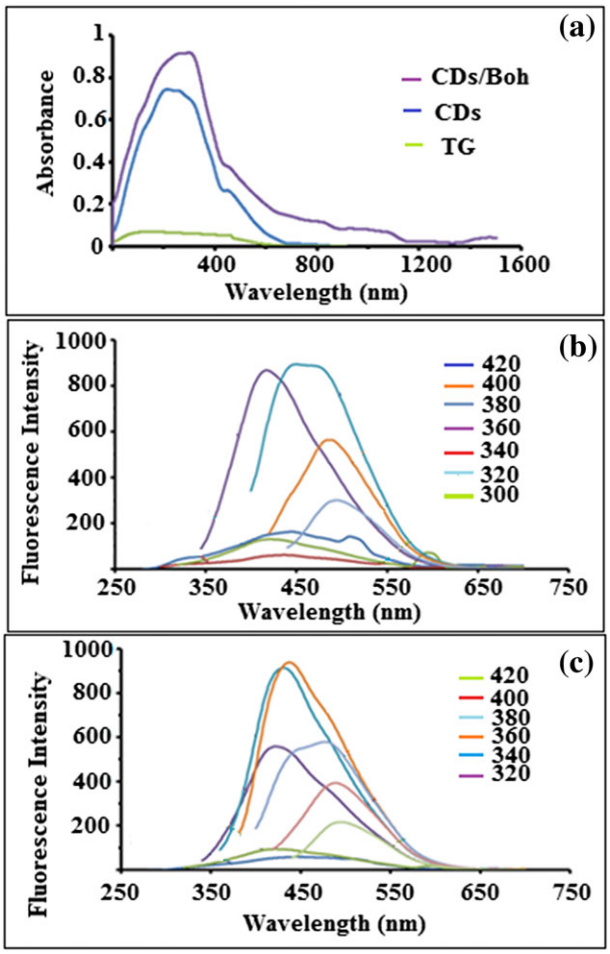

FIGURE 1 The UV-vis absorption spectrum of CDs/Boh, CDs and TG in the solvent water (a). The fluorescence spectrum of CDs in the wavelength range of 260 to 420 nm (b). The fluorescence spectrum of CDs/Boh in the wavelength range of 280 to 420 nm (c)

3.1.2 | TEM and DLS

The physical specifications of the prepared CDs were analyzed by TEM and DLS. The TEM images of CDs indicate that the prepared CDs have a spherical form and a diameter of about 4 nm (Figure 2a), these results confirm the results of the DLS method, where diameters of 1.5 up to 7 nm were observed (Figure 2b). TEM image of Boh indicates the presence of plates with various thicknesses (Figure 2c), whereas after modifying with CDs, these nanoparticles are seen on the Boh plates (Figure 2d).

3.1.3 | FT-IR

The FT-IR spectrum of the CDs, Boh and CDs/Boh are displayed in Figure 3. As shown the CDs exhibit a broad peak at 3407 cm^{-1} correspond to the stretching vibrations of –OH.[8] The peaks at 2929 and 1600–1770 cm^{-1} are a result of the stretching vibrations of

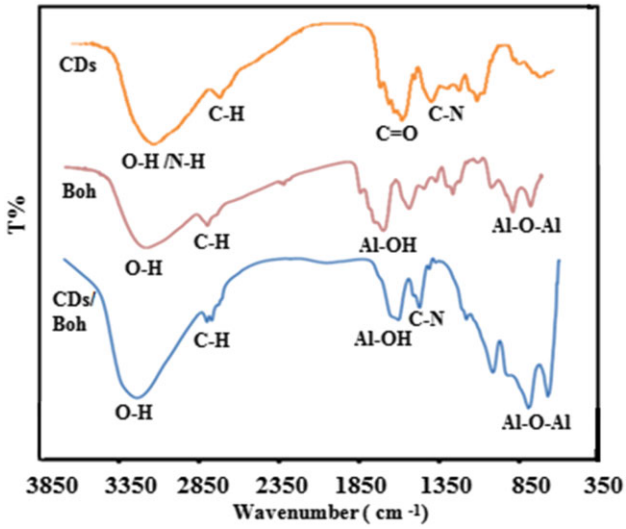

FIGURE 3 The FT-IR spectrum of synthesized CDs, CDs/Boh and Boh

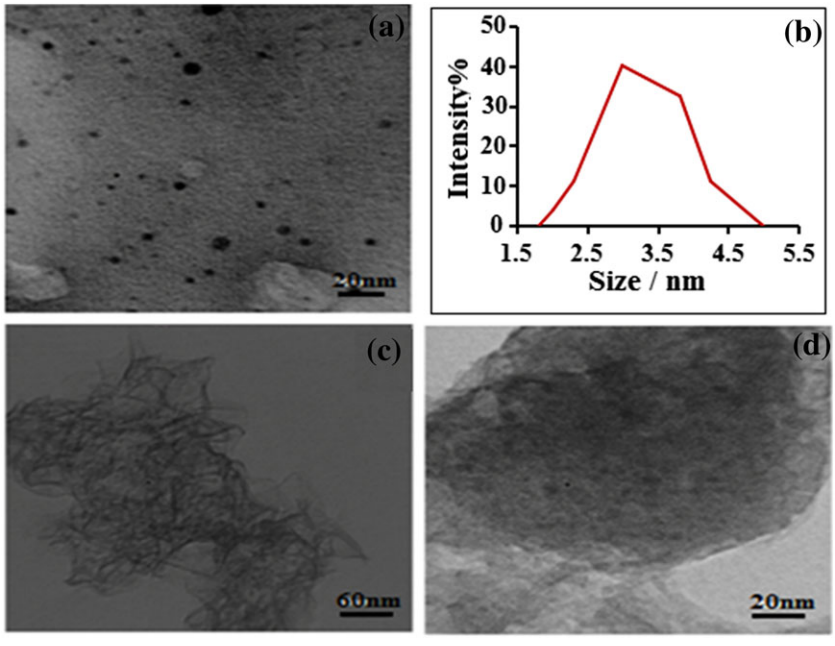

FIGURE 2 Transmission electron microscopy (TEM) images of CDs (a). DLS analysis of synthesized CDs (b). TEM image of Boh (c). TEM image of synthesized CDs/Boh (d)

–CH and C=O. In addition, the characteristic absorption peak at 1400 cm $^{-1}$ is ascribed to be owing to the presence of –C-O-H bending.[27]

To confirm the synthesis of CDs/Boh, the FT-IR spectrum is used. AlOH and Al-O-Al are two functional groups of Boh; therefore peaks are seen in the FT-IR spectrum of Boh, including stretching and bending vibrations of AlOH at 1570 cm^{-1} and 1650 cm^{-1}. Also the peak in the range from 700 to 500 cm^{-1}, relates to the Al-O-Al bands. The presence of effective groups in hydrogen bonding at the surface of CDs and Boh, confirms the formation of hydrogen bonding between them. In this way, the successful synthesis of CDs/Boh was confirmed.[28]

3.1.4 | XRD

Figure 4(a,b) displays the XRD pattern of synthesized CDs and CDs/Boh. XRD pattern was recorded during a range of 2θ (10°–100°). The XRD scheme of CDs demonstrations a wide peak at 2θ = 20° which fits to the plane (002) indicating the graphite structure of synthesized CDs.[29] In the XRD pattern of CDs/Boh the low intensity peaks at 2θ = 14/5° and 48/2° were observed, which are related to crystal structures of Boh. Moreover, a peak at 2θ = 21/4° indicates the plane (002) of CDs.[30] It can be concluded the amorphous structure of CDs/Boh formed.[18]

3.1.5 | Raman

The Raman spectrum in Figure 4(c) shows the presence of two specified peaks at 1385 cm^{-1} and 1564 cm^{-1}, respectively, related to the D band and G band. The intensity of the D band and G band is 60.2 and 68.9, respectively. The comparative intensity (I_D/I_G) for the synthesized CDs was 0.87, so these nanoparticles must have a graphite structure.[31]

3.1.6 | EDX

As shown in Figure 5(a), The major elements constituent of the synthesized CDs are carbon (63.94%) and oxygen (23.5%). Figure 5 b shows carbon, oxygen, and aluminum are the main elements of CDs/Boh.

It is noteworthy that, on the basis of the results of TEM, XRD, EDX and FT-IR characterizations, it displays that CDs/Boh were successfully synthesized.

3.1.7 | Cell viability assay

The biocompatibility of the as-synthesized CDs was investigated through assessing the viability of HeLa (cervical cancer cells) and HepG2 (liver cancer cells) cells. MTT can be reduced by live cells to form a purple formazan crystalline in a ratio to the number of viable cells. To cell evaluates (HepG2 and HeLa) 50 µL of MTT and 6.2 mg mL^{-1} CDs (treated cells) were added, hence the absorbance of treated cells were compared to the absorbance of the normal cells. Finally, the percentage of cell viability was calculated using Equation 2, MTT is light yellow in solution but generates a purple formazan product with live cells.[32] As shown in Figure 5(c), more than 85% of cells survived which indicates that the nanoparticles are not toxic.

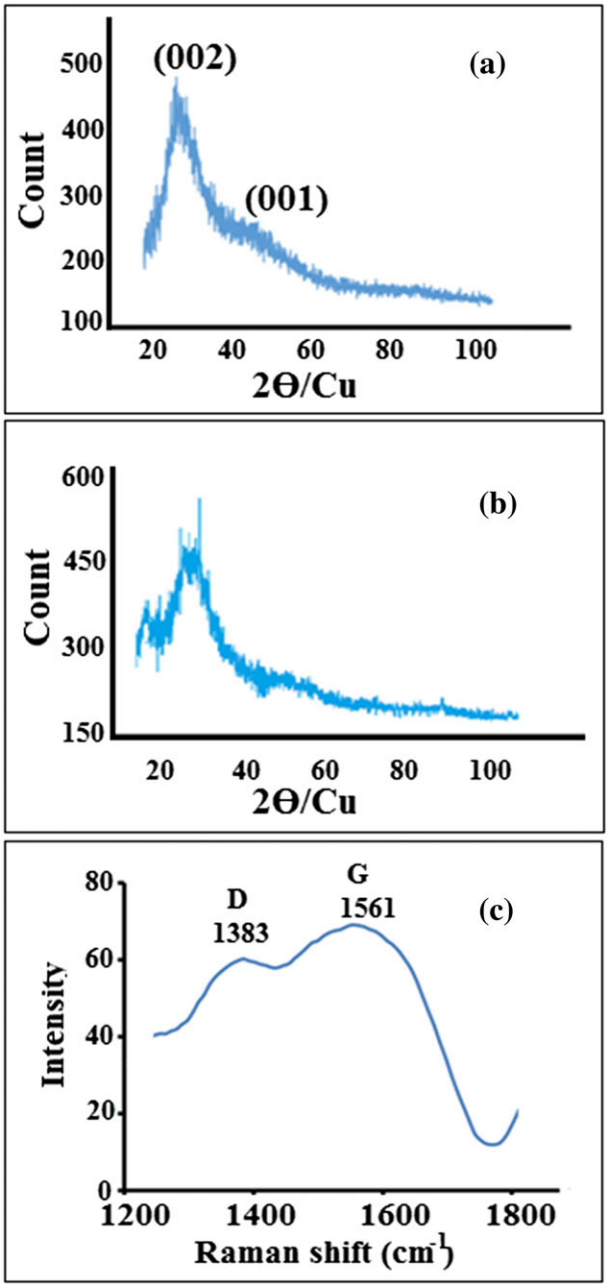

FIGURE 4 X-ray diffraction (XRD) pattern of synthesized CDs (a) and CDs/Boh (b). The Raman spectrum of synthesized CDs (c)

$$\text{Cell viability } (\%) = \frac{\text{The absorbance of test cells}}{\text{The absorbance of normal cells}} \times 100 \quad (2)$$

3.2 | Operating principles

It was quite persuasive from the TEM image (Figure 6a), which was taken after the addition of DOX to the CDs solution, that CDs–DOX aggregation occurred. The fluorescence emission of CDs could be quenched (turned-off) by the DOX drug and the red shift was observed in the emission peaks (~5 nm).

Owing to the ionized hydroxyl functional groups, the CDs are negatively charged (zeta potential: −11.0 mV). However, DOX has a positive charge due to the anthracene ring and amino group.[11]

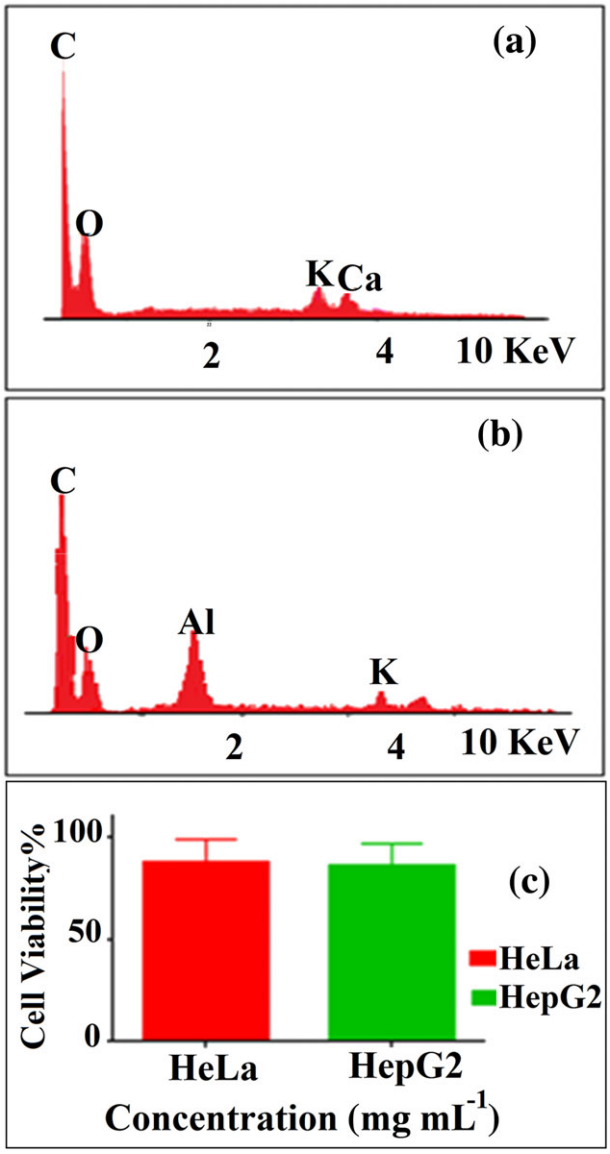

FIGURE 5 Energy dispersive X-ray (EDX) analysis of CDs (a) and CDs/Boh (b). Investigation of cell viability values (%) of two cell lines HeLa and HepG2 by MTT assay in the presence of carbon points concentrations of CDs (6.2 mg mL^{-1}) (c)

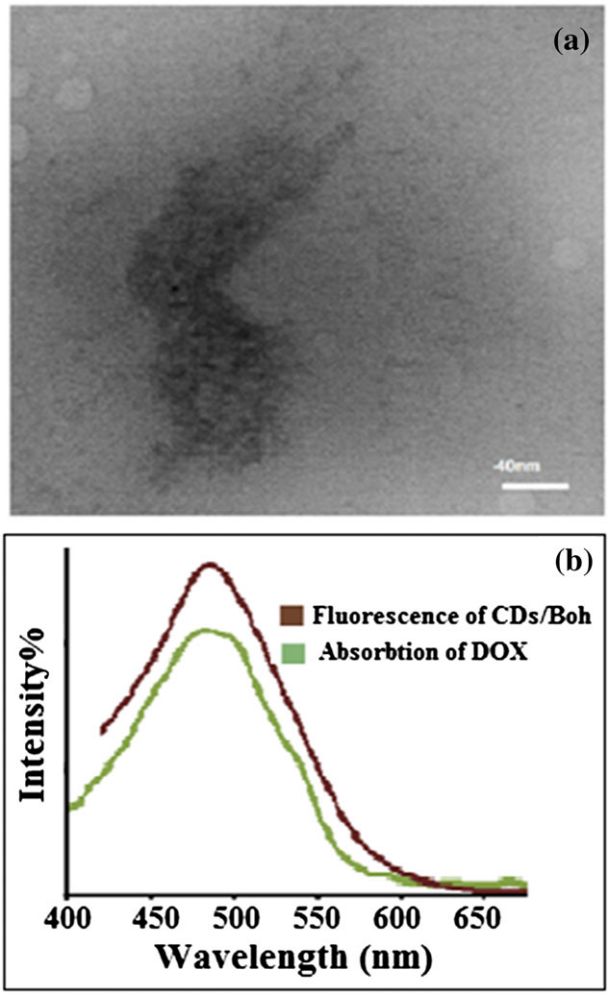

FIGURE 6 Transmission electron microscopy (TEM) images CDs with doxorubicin (DOX) addition (a). Overlap of DOX absorption spectrum and fluorescence emission spectrum of CDs/Boh (b)

Electrostatic repulsion between CDs leads to dispersion and a stable colloidal suspension is obtained. According to Scheme 2(a) with the addition of the DOX, electrostatic interaction between the CDs and the DOX cause the aggregation of the CDs and a decrease in the inter-CDs distance. Thus the aggregation strongly increases due to the energy delivery from the smaller CDs (higher energy emission) to the larger CDs (lower energy emission).[33]

With the presence of Boh modified with CDs, due to the hydrogen bonding between the CDs and AlOOH, there is no aggregation after increasing the DOX. As a result, a mechanism of IFE for the quenching of the fluorescence emotion of CDs/Boh was proposed. The mechanism of IFE happens in the case of the DOX absorption spectrum (as absorbent species) entirely covers the emission spectrum of CDs/Boh.[34] As can be seen in Figure 6(b), the absorption spectrum of DOX overlaps the emission spectrum of CDs/Boh. Due to Scheme 2(b), DOX absorbs the fluorescence emission of CDs/Boh and leads to fluorescence quenching; all conditions are in perfect correspondence with the mechanism of IFE.

3.3 | Optimizing the synthesis conditions

To optimize the synthesis conditions, different temperatures (150–280°C) and different times (2–16 h) were investigated using the hydrothermal method. The best time and temperature for the synthesis of CDs were found to be 12 h and 180°C, respectively.

3.4 | Effect of sample solution pH

The molecular structures of the DOX and CDs owing to different groups on their surfaces appeared in various anionic and cationic forms in the alkaline–acidic environment. Whereas off–on fluorescence procedure is pH-subordinate of the biosensor, to increase the sensitivity of the DOX determination, the effect of different solution pH on fluorescence properties was investigated in the presence of 120 μg mL^{-1} CDs and 100 ng mL^{-1} DOX. For this purpose, the different pH solutions were prepared in the range 3.0–12.0 and the fluorescence intensity of the biosensor was measured. As shown in Figure 7(a), in pH 5.0, the response function ($F_0 - F$) values are

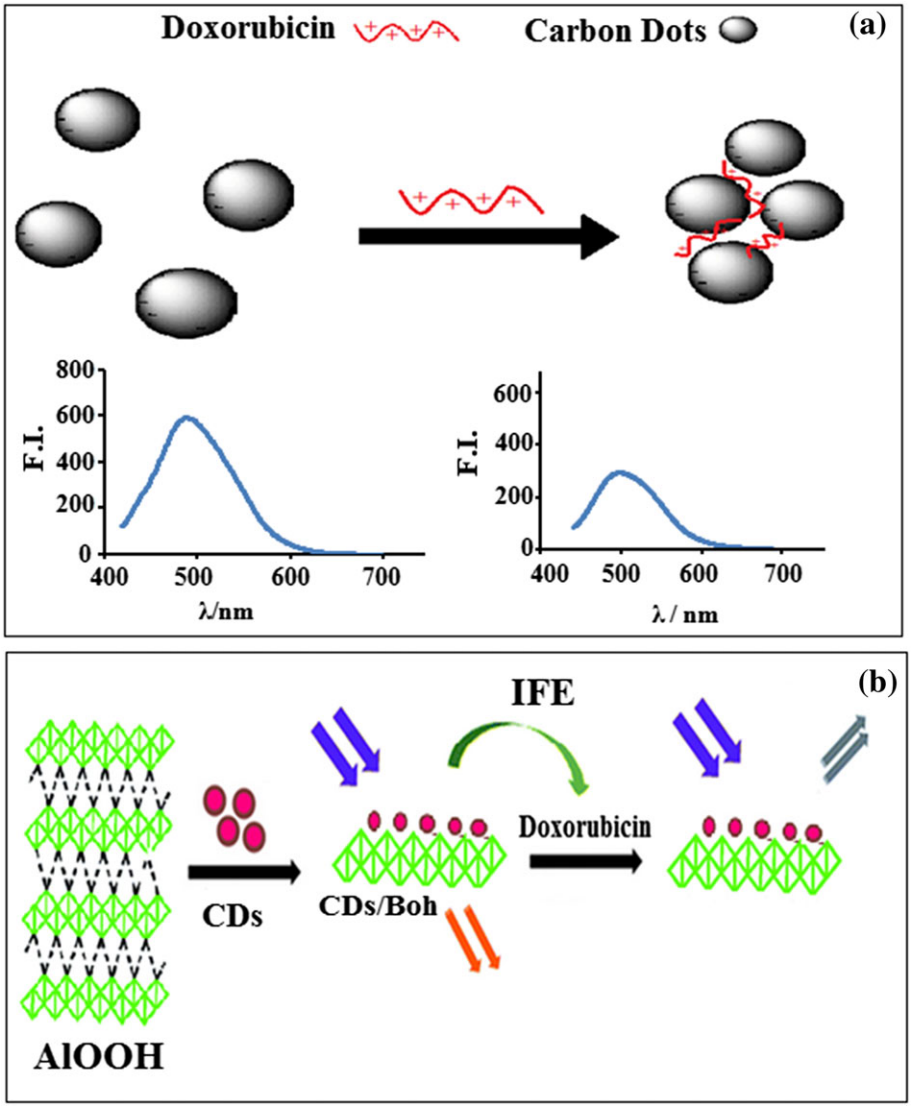

SCHEME 2 a) The quenching fluorescence of CDs after DOX addition via aggregation mechanism. b) The quenching of CDs/Boh florescence, via IFE mechanism

at a maximum, while in an alkaline environment, the response function is reduced. In fact, the pKa of the $-NH_2$ and groups in DOX are 7.2 and 9.5, respectively. The molecule (HO-DOX-NH_2) under different pH solution has different ionic forms.

In acidic pH the amino groups on the DOX are protonated thus, it has numerous positive charges (cationic DOX) and aggregation between negative CDs and DOX could occur. In neutral solutions, the DOX molecules are more in the zwitterionic form and the positive charge is decreased. However, in alkaline pH the phenol group on the DOX is deprotonated and it carries a negative charge (anionic DOX), which can decrease the interaction between CDs and DOX in alkaline pH. So, pH 5 was chosen as the best pH for further experiments.[35] As presented in Figure 7(a), for the CDs/Boh the change of fluorescence was not observed at different pH values. The changes in the intensity of fluorescence of CDs are due to the deprotonation of functional groups, including oxygen atoms in alkaline condition, it is important to note that the hydrogen bonds between the AlOOH and the oxygen group on the surface of CDs prevent the protonation and deprotonation of CDs at various pH.[29] Consequently, the different pH values were not effective in the response factor, thus, in the following steps pH 7 was used as optimal pH.

3.5 | Effect of the amount of CDs

Figure 7(b) represents the fluorescence spectra of different amounts of CDs in the existence of 100 ng mL^{-1} DOX at pH 5. The fluorescence intensity is influenced by the different concentrations of CDs and effects of the biosensor sensitivity. Experimental results illustrated that an optimum concentration of the CDs is 120 μg mL^{-1}, the lower concentration of CDs reduced the sensitivity of the biosensor and the linear calibration range and high concentrations may lead to self-absorption which decreases the fluorescence intensity.[36]

3.6 | The response time of biosensor

To evaluate the kinetics between CDs and DOX, we studied the response time of the biosensor. As presented in Figure 7(c) under optimum conditions, the fluorescence signal was measured after the

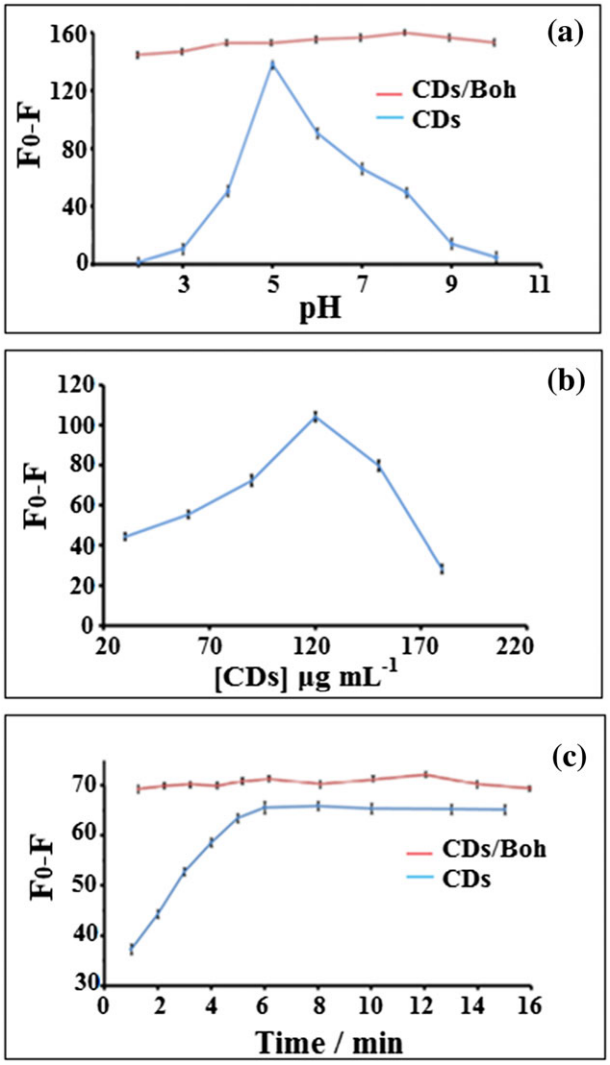

FIGURE 7 Optimization of pH for sensor of CDs in the presence of 40 µL CDs (6.2 mg mL^{-1}), 100 ng mL^{-1}DOX, influence of pH on the sensor of CDs/Boh conditions:100 ng mL^{-1} CDs/Boh and 70 ng mL^{-1} DOX (a). Effect of the concentration of CDs on the response of the sensor conditions: 100 ng mL^{-1} DOX, pH 5 and different amount of CDs (b). Optimization of time for biosensor of CDs in the presence of: 40 µL CDs (6.2 mg mL^{-1}), 100 ng mL^{-1}DOX and pH 5 and effect of time on the biosensor of CDs/Boh. Conditions: 100 ng mL^{-1} CDs/Boh, 70 ng mL^{-1} DOX and pH 5 (c)

addition of DOX and $F_0 - F$ increased within 6 min, however, the reaction time of CDs/Boh has no effect on the intensity of the fluorescence.

4 | ANALYTICAL FIGURES OF MERIT

4.1 | CDs

In the optimal situations explained earlier, the fluorescence emotion spectra of CDs in the attendance of various concentrations of DOX were recorded (Figure 8a). The response function($F_0 - F$), the quantity of this sensor, versus log*C* (C:DOX concentration) was found in the linear range of 1 to 400 ng mL^{-1} DOX by a correlation coefficient of 0.994. The theoretical limit of detection was calculated to

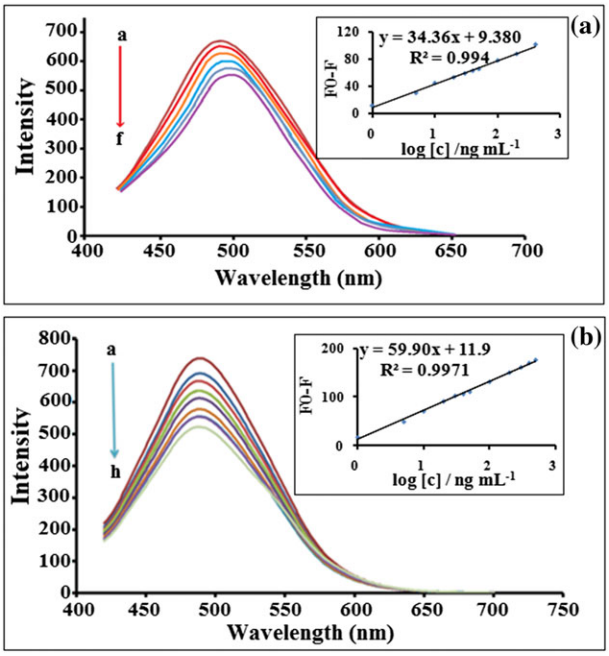

FIGURE 8 Calibration curve of CDs (6.2 mg mL^{-1}) under optimum conditions [irradiance wavelength of 400 nm at pH 0.5 under various concentrations of doxorubicin (1–400 ng mL^{-1})] (a). Calibration curve of CDs/Boh in the linear range of 1 to 500 ng mL^{-1} for the optimum conditions of 100 ng mL^{-1} CDs/Boh in the presence of a general buffer of pH 7 (b)

be 0.4 ng mL^{-1} based on ten replicates of the standard deviation of the blank. For the precision of the method, relative standard deviations based on five replicates were obtained for 10 (2.1%) and 200 (1.4%) ng mL^{-1} DOX, respectively.

4.2 | CDs/Boh

After the optimization, the optical sensor calibration curve was recorded under optimal conditions for different concentrations of DOX in the attendance of 100 ng mL^{-1} CDs/Boh and pH 7. With regard to the results obtained in Figure 8(b), the optical sensor response has a linear relationship with the log of the concentration of DOX in the range of 1 to 500 ng mL^{-1}. The detection limit of the proposed method was calculated for ten times of 0.2 ng mL^{-1}. The correlation coefficient of 0.997 was obtained. The relative standard deviations for two concentrations 20 and 150 ng mL^{-1} were obtained 1.3% and 0.9%, respectively. These values represent the acceptable repeatability for the proposed method.

5 | INTERFERENCE STUDY

The fluorescence response of CDs–DOX to various species commonly found in the blood such as K^+, Mg^{2+}, Fe^{3+}, Ca^{2+}, dopamine, ascorbic acid, uric acid, lucin, histidine, glycine, dopamine, glucose and Prednisone drug that is used in combination with DOX were chosen to appraise the selectivity of the biosensor. The different solutions including 5 µg mL^{-1} of species, 100 ng mL^{-1} DOX, and 120 µg mL^{-1}CDs were tested. As shown in Figure 9 the biosensor proves to be

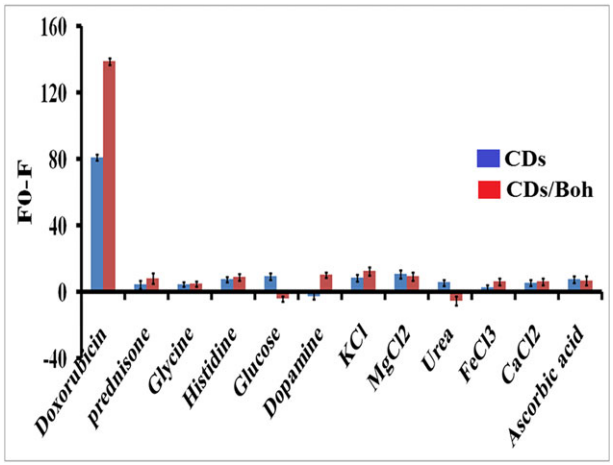

FIGURE 9 Sensor response to doxorubicin and each of the possible indifferent species in optimal conditions

a good detector for DOX. In fact, DOX is a positive charge molecule,[29] therefore the positive charge of the other tested cations were less than DOX or neutral/negative, thus leading to weaker electrostatic interactions with the CDs versus DOX. Consequently, additional neutral materials or cations have no effect on the aggregation of CDs.[18]

Owing to the hydrogen bonding between CDs/Boh and DOX electrostatic interaction between cations and CDs were reduced.[28] To appraise the selectivity of the CDs/Boh of the sensor, the sensor response in optical conditions (100 ng mL^{-1} CDs/Boh and 70 ng mL^{-1} DOX) and each of the different interference species at a concentration of 7 μg L^{-1} were recorded. The absorption spectra of the interference species did not overlap with the emission and absorption spectrum of our fluorescence species. Figure 9 shows the responses of the sensors to the interfering species.

6 | APPLICATION

The applicability and reliability of biosensors were investigated using them for the determination of DOX-spiked in the blood filtered serum samples by the procedure of the standard addition. Table 1 show that the recoveries were acceptable. The results indicated that the proposed biosensors are reliable for determination of DOX in real samples.

TABLE 1 Determinations of doxorubicin (DOX) in serum samples for CDs and CDs/Boh of sensors

Sample		DOX added (ng mL^{-1})	DOX found, proposed biosensor (ng mL^{-1})	Recovery (%)
CDs	A	50.0	51.4 ± 2	102.8 ± 3.5
		100.0	101.9 ± 3.1	101.9 ± 4.1
	B	50.0	51.8 ± 2.7	103.6 ± 5.4
		100.0	99.2 ± 3.4	99.2 ± 4.4
CDs/Boh	A	120.0	122.1 ± 3.2	101.8 ± 2.7
		350.0	355.2 ± 2.2	101.6 ± 1.9
	B	30.0	35.7 ± 3.6	119.1 ± 3.5
		180.0	188.2 ± 1.2	104.5 ± 1.4
	C	30.0	34.7 ± 1.7	115.7 ± 1.5
		180.0	187.3 ± 3.8	104.1 ± 4.1

TABLE 2 Comparison of different methods used to determine doxorubicin

Method	Linear dynamic range (ng mL^{-1})	Detection limit (ng mL^{-1})	Reference
Spectrophotometry	20–1000	6.1	[37]
Spectrophotometry	10–500	0.9	[38]
Spectrophotometry	2–500	0.5	[39]
Spectrophotometry	100–7000	30	[13]
Fluorimetry, CDs	1–400	0.4	This work
Fluorimetry, CDs/Boh	1–500	0.2	This work

7 | CONCLUSIONS

In this study, CDs were synthesized from TG for the first time. These CDs were applied as a facile optical sensor for determination of DOX based on the electrostatic aggregation of CDs. The aggregation through electrostatic interactions between CDs (negative charge) and DOX (positive charge) occurs. As a result, the repulsive force decreases between the particles and agglomeration particles are formed.[21] This mechanism was proven by TEM images and zeta potential. The detection limit of the proposed sensor was calculated at 0.4 ng mL^{-1}. In the next section of the project, the CDs/Boh was used to determine DOX. Using the Boh as the support for the CDs, lead to many advantages, such as increasing the PL stability, sensitivity, the selectivity and the compatibility of the CDs. The proposed mechanism for this optical sensor was IFE, because of the overlapping of the absorption spectra of the DOX and the CDs/Boh emission spectrum, lead to DOX operating as a strong quencher. The DOX is recognized based on the formation absorber species; as a result, fluorescence intensity and absorption change.[34] The light absorbed by the DOX in the range 400–700 nm, prevented the excitation of the CDs and subsequently reduced the fluorescence emission. Under optimal conditions, the detection limit of the method is calculated to be 0.2 ng mL^{-1}. Table 2 shows the comparison of the method used for determination of DOX with methods performed in recent years. As novel works, two sensors introduced, indicate two economies, simple, rapid and good fluorescence sensors efficiency for the detection of DOX.

ACKNOWLEDGEMENTS

Sincere thanks to Isfahan University of Technology (IUT) Research Council, Center of Excellence in Sensor and Green Chemistry for their support.

ORCID

Behzad Rezaei http://orcid.org/0000-0003-0055-0486

REFERENCES

[1] J. Zuo, T. Jiang, X. Zhao, X. Xiong, S. Xiao, Z. Zhu, *J. Nanomater.* **2015**, *10*.

[2] W. Zhou, S. Dong, Y. Lin, C. Lu, *Chem. Commun.* **2017**, *53*, 2122.

[3] L. Wang, H. S. Zhou, *Anal. Chem.* **2014**, *86*, 8902.

[4] Z. A. Qiao, Y. Wang, Y. Gao, H. Li, T. Dai, Y. Liu, Q. Huo, *Chem. Commun.* **2010**, *46*, 8812.

[5] Y. P. Sun, B. Zhou, Y. Lin, W. Wang, K. S. Fernando, P. Pathak, M. J. Meziani, B. A. Harruff, X. Wang, H. Wang, *J. Am. Chem. Soc.* **2006**, *128*, 7756.

[6] B. De, N. Karak, *RSC Adv.* **2013**, *3*, 8286.

[7] Y. Liu, Q. Zhou, J. Li, M. Lei, X. Yan, *Sens. Actuators B* **2016**, *237*, 597.

[8] M. Darroudi, M. Sarani, R. K. Oskuee, A. K. Zak, M. S. Amiri, *Ceram. Int.* **2014**, *40*, 2863.

[9] S. Balaghi, M. A. Mohammadifar, A. Zargaraan, H. A. Gavlighi, M. Mohammadi, *Food Hydrocoll.* **2011**, *25*, 1775.

[10] B. Wang, S. Wang, Y. Wang, Y. Lv, H. Wu, X. Ma, M. Tan, *Biotechnol. Lett.* **2016**, *38*, 191.

[11] Q. Wang, X. Huang, Y. Long, X. Wang, H. Zhang, R. Zhu, L. Liang, P. Teng, H. Zheng, *Carbon* **2013**, *59*, 192.

[12] G. Wei, S. Xiao, D. Si, C. Liu, *Biomed. Chromatogr.* **2008**, *22*, 1252.

[13] H. Tavallali, A. Jahanbekam, *Int J Pharm Tech Res.* **2010**, *2*, 1943.

[14] J. Fei, X. Wen, Y. Zhang, L. Yi, X. Chen, H. Cao, *Microchim. Acta* **2009**, *164*, 85.

[15] A. Gavenda, J. Ševčík, J. Psotová, P. Bednář, P. Barták, P. Adamovský, V. Šimánek, *Electrophoresis* **2782**, *2001*, 22.

[16] Y. Guo, Y. Chen, Q. Zhao, S. Shuang, C. Dong, *Electroanalysis* **2011**, *23*, 2400.

[17] S. Dong, Z. Yuan, L. Zhang, Y. Lin, C. Lu, *Anal. Chem.* **2017**, *89*, 12520.

[18] G. Mohammadnezhad, O. Akintola, W. Plass, F. Steiniger, M. Westermann, *Dalton Trans.* **2016**, *45*, 6329.

[19] P. Yuan, D. R. Walt, *Anal. Chem.* **1987**, *59*, 2391.

[20] A. D. McNaught, A. Wilkinson, *Lippman's Equation*, 2nd ed., Blackwell Science, Oxford, UK **1997**.

[21] M. Noh, T. Kim, H. Lee, C. K. Kim, S. W. Joo, K. Lee, *Physicochem Eng Asp.* **2010**, *359*, 39.

[22] Y. He, J. He, H. Zhang, Y. Liu, B. Lei, *J. Colloid Interface Sci.* **2017**, *496*, 8.

[23] J. Zong, Y. Zhu, X. Yang, J. Shen, C. Li, *Chem. Commun.* **2011**, *47*, 764.

[24] S. Zhu, Y. Song, X. Zhao, J. Shao, J. Zhang, B. Yang, *Nano Res.* **2015**, *8*, 355.

[25] D. Kaushik, G. Bansal, *J. Pharmaceut. Anal.* **2015**, *5*, 285.

[26] S. Li, S. Zhou, H. Xu, L. Xiao, Y. Wang, H. Shen, H. Wang, Q. Yuan, *J. Mater. Sci.* **2016**, *51*, 6801.

[27] R. M. Shereema, V. Sankar, K. G. Raghu, T. P. Rao, S. S. Shankar, *Electrochim. Acta* **2015**, *182*, 588.

[29] T. N. Edison, R. Atchudan, M. G. Sethuraman, J. J. Shim, Y. R. Lee, *J. Photochem. Photobiol. B.* **2016**, *161*, 154.

[30] R. Pourfaraj, S. J. Fatemi, S. Y. Kazemi, P. Biparva, *J. Colloid Interface Sci.* **2017**, *508*, 65.

[31] M. Fan, C. Zhu, J. Yang, D. Sun, *Electrochim. Acta* **2016**, *216*, 102.

[32] A. Kumar, S. Selvakumar, *Pharmacogn. Mag.* **2015**, *11*, S46.

[33] S. F. Wuister, I. Swart, F. van Driel, S. G. Hickey, *Nano Lett.* **2003**, *3*, 503.

[34] M. Zheng, Z. Xie, D. Qu, D. Li, P. Du, X. Jing, Z. Sun, *ACS Appl. Mater. Interfaces* **2013**, *5*, 13242.

[35] T. Sun, M. Zheng, Z. Xie, X. Jing, *Mater Chem Front.* **2017**, *1*, 354.

[36] B. Rezaei, M. Shahshahanipour, A. A. Ensafi, *Mater. Sci. Eng. C* **2017**, *71*, 663.

[37] B. Gnapareddy, S. R. Dugasani, T. Ha, B. Paulson, T. Hwang, T. Kim, J. H. Kim, K. Oh, S. H. Park, *Sci. Rep.* **2015**, *5*, 12722.

[38] T. Pérez-Ruiz, C. Martínez-Lozano, A. Sanz, E. Bravo, *Electrophoresis* **2001**, *22*, 134.

[39] H. C. Yao, E. J. Xu, W. Y. Zeng, X. Y. Zeng, M. Zhang, J. Chen, *J. Food. Drug. Anal.* **2013**, *21*, 279.

How to cite this article: Rezaei B, Hassani Z, Shahshahanipour M, Ensafi AA, Mohammadnezhad G. Application of modified mesoporous boehmite (γ-AlOOH) with green synthesis carbon quantum dots for a fabrication biosensor to determine trace amounts of doxorubicin. *Luminescence.* 2018;1–10. https://doi.org/10.1002/bio.3558